



ARL-TR-8991 • JULY 2020



Preliminary Results for the Incorporation of Peptides into the Traditional Lateral Flow Assay

by Wais Mojadedi, Alexander Winton, and Matthew Coppock

NOTICES

Disclaimers

The findings in this report are not to be construed as an official Department of the Army position unless so designated by other authorized documents.

Citation of manufacturer's or trade names does not constitute an official endorsement or approval of the use thereof.

Destroy this report when it is no longer needed. Do not return it to the originator.



Preliminary Results for the Incorporation of Peptides into the Traditional Lateral Flow Assay

Wais Mojadedi

Oak Ridge Associated Universities

Alexander Winton and Matthew Coppock

Sensors and Electron Devices Directorate, CCDC Army Research Laboratory

REPORT DOCUMENTATION PAGE

Form Approved
OMB No. 0704-0188

Public reporting burden for this collection of information is estimated to average 1 hour per response, including the time for reviewing instructions, searching existing data sources, gathering and maintaining the data needed, and completing and reviewing the collection information. Send comments regarding this burden estimate or any other aspect of this collection of information, including suggestions for reducing the burden, to Department of Defense, Washington Headquarters Services, Directorate for Information Operations and Reports (0704-0188), 1215 Jefferson Davis Highway, Suite 1204, Arlington, VA 22202-4302. Respondents should be aware that notwithstanding any other provision of law, no person shall be subject to any penalty for failing to comply with a collection of information if it does not display a currently valid OMB control number.

PLEASE DO NOT RETURN YOUR FORM TO THE ABOVE ADDRESS.

1. REPORT DATE (DD-MM-YYYY) July 2020		2. REPORT TYPE Technical Report		3. DATES COVERED (From - To) January 2019–May 2020	
4. TITLE AND SUBTITLE Preliminary Results for the Incorporation of Peptides into the Traditional Lateral Flow Assay				5a. CONTRACT NUMBER	
				5b. GRANT NUMBER	
				5c. PROGRAM ELEMENT NUMBER	
6. AUTHOR(S) Wais Mojadedi, Alexander Winton, and Matthew Coppock				5d. PROJECT NUMBER	
				5e. TASK NUMBER	
				5f. WORK UNIT NUMBER	
7. PERFORMING ORGANIZATION NAME(S) AND ADDRESS(ES) CCDC Army Research Laboratory ATTN: FCDD-RLS-CB Adelphi, MD 20783				8. PERFORMING ORGANIZATION REPORT NUMBER ARL-TR-8991	
9. SPONSORING/MONITORING AGENCY NAME(S) AND ADDRESS(ES)				10. SPONSOR/MONITOR'S ACRONYM(S)	
				11. SPONSOR/MONITOR'S REPORT NUMBER(S)	
12. DISTRIBUTION/AVAILABILITY STATEMENT Approved for public release; distribution is unlimited.					
13. SUPPLEMENTARY NOTES ORCID IDs: Matthew B Coppock, 0000-0001-9305-3846; Alexander J Winton, 0000-0002-4591-1655					
14. ABSTRACT The lateral flow immunoassay (LFA) is a robust, rapid point-of-care test used to detect specific molecules in biological samples. They hold significant advantages for use in the US Army, including monitoring of warfighter health and performance as well as providing the ability to test for hazardous foreign substances in the field. The traditional LFA uses antibodies as biorecognition elements, which can limit the shelf-life and operational functionality of the assay due to the poor thermostability exhibited by antibodies. Additionally, significant time is required to manufacture antibodies. As an alternative for antibodies, peptides are capable of comparable performance but with added stability and ease of production. In this report we investigate some of the considerations required to facilitate incorporation of peptides into the LFA using streptavidin-binding-peptide as the model reagent.					
15. SUBJECT TERMS lateral flow assay, LFA, antibody alternatives, protein catalyzed capture agents, biosensing					
16. SECURITY CLASSIFICATION OF:			17. LIMITATION OF ABSTRACT UU	18. NUMBER OF PAGES 33	19a. NAME OF RESPONSIBLE PERSON Matthew Coppock
a. REPORT Unclassified	b. ABSTRACT Unclassified	c. THIS PAGE Unclassified			19b. TELEPHONE NUMBER (Include area code) 301-394-5520

Contents

List of Figures	iv
List of Tables	v
1. Introduction	1
2. Materials	5
2.1 LFA Components	5
2.2 Reagents	5
2.3 Instrumentation	6
3. Methods	6
3.1 Preparation of Gold Nanoparticles	6
3.2 Conjugation of Gold Nanoparticles	7
3.3 Conjugation of Red Carboxylate Latex Beads	7
3.4 Test-Line Modification	8
3.4.1 Passive Adsorption	8
3.4.2 Covalent Linking Strategy	8
3.5 LFA Preparation and Assembly	8
3.6 Dipstick Assays	9
4. Results and Discussion	9
4.1 Covalent Immobilization of Biotin	9
4.2 Investigation of Passive Adsorption	11
4.3 Characterization of Red-Carboxylate Latex Beads	13
4.4 Characterization of AuNPs	16
5. Conclusion	20
6. References	21
List of Symbols, Abbreviations, and Acronyms	24
Distribution List	26

List of Figures

Fig. 1	Components and principle of the LFA. (Reproduced with permission under a Creative Commons License 4.0).....	2
Fig. 2	General reaction scheme for a copper(I) catalyzed click reaction.....	9
Fig. 3	General schematic depicting the pathway used for covalent modification at the test-line surface of nitrocellulose.....	10
Fig. 4	Results from the covalent immobilization of ligands and in situ click reaction at the test line of nitrocellulose using DVS. Chemiluminescence was measured after probing with streptavidin-HRP and developing the signal using a SuperSignal substrate.....	10
Fig. 5	Capture of red-streptavidin latex beads by small biotinylated molecules (MW<1000 g/mol) that were passively adsorbed to the test-line surface: A) GTP-biotin at 2.5 mM, B) HS-SBP at 100 mM, C) NHS-biotin at 10 mM, and D) NHS-biotin at 1 mM.....	11
Fig. 6	Red-streptavidin latex beads captured by (left) an anti-streptavidin antibody and (right) HS-SBP ranging from pH 5 to pH 9 (top to bottom).....	12
Fig. 7	Layering of (left) NHS-biotin and (right) HS-SBP. A control is included in the first row (BSA at the test line for NHS-biotin and red-COOH unfunctionalized beads for HS-SBP). Stock concentrations were 10 and 100 mM for NHS-biotin and HS-SBP, respectively. Layering is shown from one to four layers (top to bottom).....	13
Fig. 8	(top) Streptavidin used to capture red-SBP reporter, deposited at 187 μ M. (bottom) Sandwich assay detecting streptavidin at 1 μ M using a red-SBP reporter and anti-streptavidin antibody as the capture agent.	14
Fig. 9	Evaluation of nonspecific binding by native, unmodified carboxylate beads. Native beads appear to have affinity for His-tagged constructs (right).	14
Fig. 10	Evaluation of nonspecific binding of native red carboxylate beads to a His-tagged construct from (left) pH 2 through pH 6, and (right) pH 7 through pH 12	15
Fig. 11	Evaluation of various measures taken to mitigate nonspecific binding of red latex beads to a His-tagged construct. (left to right) Each column consists of nSP1-His6 at 1, 10, and 20 μ M. The top row is a control, the middle row includes the addition of 100-mM imidazole, and the bottom row includes the addition of 100-mM CaCl ₂	15
Fig. 12	Prevention of nonspecific binding of unmodified native latex beads to CcpA-His ₆ using cobalt (II) chloride as a divalent cation inhibitor at (top to bottom) 100, 500, and 1.0 M.	16
Fig. 13	Capture of citrate-capped native 40-nm AuNP's using CcpA-His ₆ , HprK-His ₆ , and nSP1-His ₆	17

Fig. 14	A) Ligand concentration screen for functionalization of AuNPs with HS-PEG-biotin MW5000. B) pH stability screen of native AuNPs. ...	18
Fig. 15	Capture of AuNP-S-PEG-biotin MW5000 reporter using (top to bottom) streptavidin at 187 μ M, streptavidin at 18.7 μ M, sandwich assay detecting 1- μ M streptavidin using anti-streptavidin as a capture agent, and sandwich assay detecting 1- μ M streptavidin using SBP as a capture agent	18
Fig. 16	A) Evaluation of nonspecific binding to nSP1-His ₆ by AuNP-S-PEG-biotin MW1000 using various blockers and ligand:blocker ratios. B) Evaluation of intended target binding using streptavidin as a capture agent to bind AuNP-S-PEG-biotin MW1000 using those same blockers and ligand:blocker ratios.	19
Fig. 17	A) Evaluation of nonspecific binding to nSP1-His ₆ by AuNP-S-SBP using various blockers and ligand:blocker ratios. B) Evaluation of intended target binding using streptavidin as a capture agent to bind AuNP-S-SBP using those same blockers and ligand:blocker ratios. ...	20

List of Tables

Table 1	Properties of some antibody mimetics that have been developed	3
Table 2	Small compounds chosen to be passively adsorbed to the test line	11

1. Introduction

The lateral flow assay (LFA) is a simple paper-based test that enables the rapid visual detection of specific biomolecules in a complex sample matrix. Industrial use of LFAs has been vast over the years, including practical applications in point-of-care (POC) clinical diagnostics,¹ pathogen identification,^{2,3} biomarker detection,⁴ and food safety evaluation,⁵ among others. Since its first introduction to the industry in the 1980s and 1990s, the LFA has continued to evolve into a multibillion-dollar industry.⁶ In 2006 alone, more than 200 companies worldwide were involved in the development of LFAs for various applications with an estimated value of \$2.1 billion.⁶ The industrial gravitation has continued to increase, likely as the result of the significant underlying advantages of the LFA, including low cost of production, little waste generation, and ease of use compared with traditional biodetection modalities.⁷ These advantages are particularly promising for Army operational environments and can enhance the effectiveness of the warfighter by assisting with decision making in regards to Soldier health and performance and allowing the rapid identification of potentially hazardous foreign substances in the field without the burden of heavy gear or the accumulation of chemical waste products.

Structurally, the LFA is composed of four distinct paper components assembled in an overlapping fashion to ensure continuity of the flow path against a plastic backing. An example of a LFA is shown in Fig. 1.

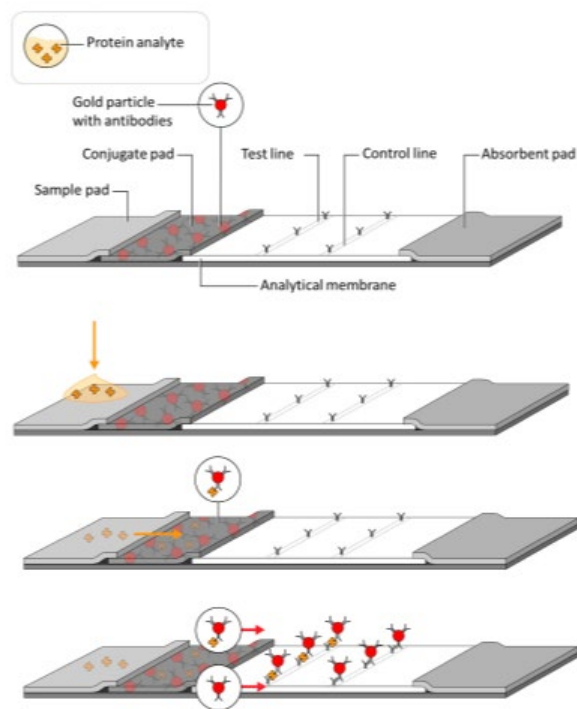


Fig. 1 Components and principle of the LFA⁸ (reproduced with permission under a Creative Commons License 4.0)

The first element is the sample pad, which, as the name suggests, is where the sample of interest is introduced, flowing through the paper via capillary action. As the analyte leaves the sample pad it contacts the second element, the conjugate pad, where a reporter is housed. This reporter remains embedded in the conjugate pad and is tethered to an antibody that is specific to a target analyte potentially in the sample. Upon resuspension by the matrix flow, the analyte becomes labeled with the detectable reporter through interaction with the antibody. As this analyte–reporter complex migrates, it is transitioned over to the third element, the porous nitrocellulose membrane, where the labeled analyte migrates and is captured by a second antibody deposited downstream at a site commonly referred to as the test line. The fourth element, known as the absorbent pad, is used as a reservoir for fluid collection and helps drive capillary action by preventing saturation of the paper components.

Each of the elements in the LFA can be customized to accommodate different applications and optimized to meet the user-defined performance expectations. Modifications can be made to the sample matrix, predried buffer composition, reporter types, and nitrocellulose pore size, among others. While this versatility makes the LFA quite promising and robust, it also lends itself to increasing complexity given the sheer number of possible variations.

Antibodies remain the gold-standard biorecognition molecules used in the traditional LFA for labeling and capturing targets. This is primarily because of the strong, highly specific binding interaction antibodies have with their respective antigens. However, there are limitations associated with antibodies, including the time-consuming production process, batch-to-batch variability, and poor thermostability, all of which can diminish the efficacy of LFA in the field. To maintain appropriate functionality of the assay in various environments, it is necessary to incorporate capture agents that are not susceptible to the confines posed by traditional antibodies.

To address the shortcomings of antibodies, many different classes of nonimmunoglobulin (non-Ig) biosensors have been developed over the years.⁹ Some non-Ig affinity ligands include affimers, affinity clamps, aptamers, avimers, DARPins, fluctuation-regulated affinity proteins, knottins, monobodies, and protein-catalyzed capture agents (PCCs). General properties of these molecules are shown in Table 1. Most non-Ig affinity ligands are produced using the common strategy of tethering variable binding motifs to small, stable, protein-based scaffolds.⁹⁻¹¹ Thus, by producing a library of stable scaffolds with random diverse binding motifs, and subsequently screening these compounds against a target, novel binding domains can be elucidated. Given the majority of non-Ig affinity ligands retain an amino acid foundation, have low molecular weights, and generally lack intricate secondary structure,^{10,11} we investigated the efficacy of integrating peptides, which exhibit similar properties, into the LFA.

Table 1 Properties of some antibody mimetics that have been developed

Antibody alternative	Structural components	Production strategy	Reference
Affimer	Protease inhibitor scaffold with variable (nine amino acids) presenting region used to generate a diverse library for screening against targets	Genetic engineering and expression in bacterial culture (E. coli)	Kyle ¹² Klont et al. ¹³
Affinity clamp	Enhancer linked to a known peptide motif and screened against targets to generate high-affinity variants	Evolved and selected through phage display	Koide and Huang ¹⁴
Aptamer	Peptide or DNA/RNA component tethered to a protease inhibitor scaffold designed using bioinformatics	Developed using systematic evolution of ligands by exponential enrichment	Thiviyanathan and Gorenstein ¹⁵

Table 1 Properties of some antibody mimetics that have been developed (continued)

Antibody alternative	Structural components	Production strategy	Reference
Avimer	Independently folded binding domain from different cell surface receptors consisting of conserved (~35 amino acids [aa's]) and variable regions (~12 aa's) modified for targeted affinity	Genetic engineering and expression in bacterial culture (E. coli)	Simeon and Chen ¹⁰ Silverman et al. ¹⁶
DARPin	Native ankyrin repeats of 33 aa's contain seven variable residues from which a library is prepared and screened against targets	Genetic engineering and expression in bacterial culture (E. coli)	Stumpp et al. ¹⁷
Fluctuation-regulated affinity proteins	After computational assessment, the antigen binding pocket of an antibody is grafted to a non-Ig scaffold to essentially mimic a truncated antibody	In silico preselection of antigen binding pockets, followed by genetic engineering and expression in bacterial culture (E. coli)	Kadonosono et al. ¹⁸
Knottin	Exceptionally stable 30-residue protein fold with several surface-exposed loops substituted with ligand binding motifs	In vitro peptide synthesis followed by oxidation to yield cysteine crosslinking	Simeon and Chen ¹⁰ Richards ¹¹
Monobody	Combinatorial modification of fibronectin type-III domain as a scaffold	Yeast surface display and phage display	Sha et al. ¹⁹
Protein-catalyzed capture agents	Library of fully synthetic cyclic peptides screened against synthetic epitopes and selected using click chemistry	In vitro peptide synthesis used to produce a synthetic epitope and the cyclic peptides	Coppock et. al. ^{20,21}

In this report we present the preliminary results for the integration of peptides into the LFA by using streptavidin-binding-peptide (SBP) as the model peptide. SBP was previously characterized to bind streptavidin with a dissociation constant (K_d) of 15 nM as determined by surface plasmon resonance immunoassay, which is comparable to the binding affinity of most non-Ig ligands as well as some antibodies. Additionally, SBP binds streptavidin at an allosteric site, thus preserving the biotin binding sites for use in characterizing the sandwich assay. By using SBP as a proof of concept, we can demonstrate that peptides are a viable substitute to antibodies in the LFA and pave the way for future studies implementing other non-Ig affinity ligands with real-world applications.

Perhaps the biggest consideration is the difference in size between peptides and antibodies, which can be nearly 1–3 orders of magnitude larger than most peptides.

This has implications on the test-line immobilization strategy. Traditionally, antibodies are deposited onto the surface of nitrocellulose and remain adsorbed due to the overwhelming electrostatic interactions with the positively charged surface.²² Because many peptides lack the intricate folding and secondary structure patterns to remain adhered to the nitrocellulose surface, we predicted that they would likely demonstrate mobility after being wetted at the test line by the sample flow. To assess this, we evaluated both passive adsorption and covalent linking strategies at the test line.

Furthermore, two different reporter options were explored: carboxylate-functionalized red latex beads and gold nanoparticles. The red latex bead reporter was chosen due to the vibrant, high-sensitivity signal produced at the test line in addition to the robust coupling potential made possible through the free carboxylate groups. Similarly, gold nanoparticles were also used due to the ease of generating a self-assembled monolayer using the gold–sulfur coordinate–covalent interaction, as well as their simple in-house synthesis protocol, which allows for cheap, reliable production of nanoparticles.

We characterize some of the challenges associated with incorporating peptide capture agents into the LFA with hopes of using other non-Ig affinity ligands in the same capacity. The results describe the workflow and troubleshooting of the assay performed in-house during characterization. Note that to finalize an LFA for use, assays must be taken to appropriate LFA vendors for optimization, scaling, and functional development followed by characterization of sensitivity and specificity prior to use in either diagnostics or biomolecule/organism identification.

2. Materials

2.1 LFA Components

CF4 sample pad paper (22 mm × 50 m), Standard 14 glass fiber, and FF120HP nitrocellulose rolls were obtained from GE Healthcare Life Sciences (Marlborough, Massachusetts). Plastic backing cards (80 mm wide) were obtained from DCNovations (Carlsbad, California).

2.2 Reagents

Bovine serum albumin (BSA), Tween20, sucrose, 2-(N-morpholino)ethanesulfonic acid (MES), divinyl sulfone (DVS), N,N-dimethylformamide (DMF), dimethyl

sulfoxide (DMSO), β -mercaptoethanol (β ME), EZ Link NH_2 -polyethylene glycol (PEG)₂-biotin, streptavidin from streptomyces avidinii, imidazole, calcium chloride, cobalt chloride, sodium carbonate, 1-ethyl-3-(3-dimethylaminopropyl)carbodiimide (EDC), N-hydroxysulfosuccinimide sodium salt (sulfo-NHS), mercaptoundecanoic acid (MUDA), hydrogen tetrachloroaurate(III) hydrate (HAuCl_4), and sodium citrate trihydrate (NaCt) were all obtained from Sigma-Aldrich Chemical Company (Milwaukee, Wisconsin). Amine polyethylene glycol bicyclononyne (exo) (NH_2 -PEG₃-BCN) and azido polyethylene glycol biotin (N_3 -PEG-biotin) were both purchased from Conju-Probe (San Diego, California). Biotinylated anti-streptavidin antibody was purchased from Vector Laboratories (Burlingame, California). Streptavidin-HRP conjugate and SuperSignal West Femto Maximum Sensitivity Substrate were purchased from ThermoFisher Scientific (Waltham, Massachusetts). Thiol polyethylene glycol carboxylate (HS-PEG-COOH; molecular weight (MW)5000 and MW10,000), and thiol polyethylene glycol biotin (HS-PEG-biotin; MW1000 and MW5000) were all purchased from PurePEG (San Diego, California). Red carboxylate latex beads (red-COOH) and red streptavidin latex beads (red-streptavidin) were both purchased from Bangs Laboratories (Fishers, Indiana). All chemicals purchased were American Chemical Society reagent grade, $\geq 95\%$ pure, and all solutions were prepared in 1X phosphate buffered saline (PBS) using high-performance liquid chromatography (HPLC)-grade (18.2-M Ω) water unless otherwise specified.

2.3 Instrumentation

Chemiluminescent imaging was performed using a Molecular Imager VersaDoc MP4000 obtained from Bio-Rad (Hercules, California). UV-visual data were measured and collected using a DS-11 series spectrophotometer obtained from Denovix (Wilmington, Delaware). SBP having the amino acid sequence AWRHPQGG and thiolated SBP (HS-SBP) having the amino acid sequence CAWRHPQGG were synthesized using an automated microwave peptide synthesizer, as reported in Coppock and Stratis-Cullum.²³

3. Methods

3.1 Preparation of Gold Nanoparticles

Gold nanoparticles (AuNPs) were synthesized in-house using the Turkevich method as described by Kozlowski et al.²⁴ to produce approximately 14 ± 1.4 -nm citrate-stabilized particles. Briefly, HAuCl_4 (0.0197 g; 0.0579 mmol) was dissolved in 50 mL of pure water with vigorous stirring and heated until boiling. A 5-mL

solution of 3.67-mM NaCt was then prepared and quickly added to mixture. Several transient color changes were then observed. Before the addition of NaCt, the HAuCl₄ solution was gold-colored. Following the addition of NaCt, the mixture became clear, then black, and then a vibrant purple before finally settling on a dark-red tinge. After recognition of this red hue, the reaction was timed for 15 min to ensure completion. The mixture was then allowed to cool to room temperature before being filtered through a 0.2- μ m sterile filter. The nanoparticles were kept at 4 °C until further use. Due to instrument limitations, the mean nanoparticle size was not characterized.

3.2 Conjugation of Gold Nanoparticles

Prior to functionalization, AuNPs ($OD_{535} = 3$) were washed by pelleting using centrifugation at 6000 xg for 30 min, decanting to remove any free citrate, and resuspending in an equal volume of pure water. This wash step was repeated two more times before resuspending the AuNPs in the desired functionalization solvent (which varied depending on the desired thiolated ligand solubility; usually either pure water or DMSO was used unless otherwise specified). Then the desired ligand was added to the suspension of AuNPs and allowed to functionalize overnight with agitation. To determine the ratio of ligand to AuNP, the packing density (ρ_{packing}) was computed using an average AuNP radius (r) of 60 nm:

$$\rho_{\text{packing}} = \frac{\text{ligand molecules}}{\text{AuNP surface area}} = \frac{\text{mol}_{\text{ligand}} * 6.022E23 \text{ molecules/mol}}{4\pi r^2}$$

After overnight functionalization was performed, the AuNPs were washed into LFA buffer (1.0% BSA, 0.1% Tween20 in 1X PBS, pH 7.4) for use in the assay.

3.3 Conjugation of Red Carboxylate Latex Beads

Red carboxylate latex beads were modified to bear various ligands using EDC/NHS coupling. Briefly, 0.2 mL of beads was pelleted using centrifugation at 17,000 xg for 15 min. The supernatant was decanted, and the remaining pellet was resuspended in 1 mL of coupling buffer (0.1 M MES, pH 6.0). This wash step was performed three times before resuspending to a final volume of 1-mL coupling buffer. Then EDC (prepared in water) and sulfo-NHS were added to the solution to a final concentration of 1 mg/mL each and agitated for 30 min at room temperature. The beads were then washed as done previously, resuspended in coupling buffer, combined with the desired ligand, and allowed to react for 3 h at room temperature with agitation. After 3 h the beads were washed into LFA buffer (1.0% BSA, 0.1% Tween20 in 1X PBS, pH 7.4) for use in the assay.

3.4 Test-Line Modification

3.4.1 Passive Adsorption

Passive adsorption was performed by depositing 1 μ L of ligand at the test line in a linear fashion and drying for 5 min at room temperature before use.

3.4.2 Covalent Linking Strategy

Covalent immobilization of ligands at the test line was performed by using divinyl sulfone DVS, which, as demonstrated by Lauritzen et al.,²⁵ can displace the nitro group on nitrocellulose and provide an arm for nucleophilic attack by amine-containing compounds to facilitate a covalent linkage to the surface. To maintain the same flow properties of homogenous nitrocellulose, only the test line was exposed to DVS. Briefly, a strip of nitrocellulose was first washed with pure water and dried at 37 °C for 3–5 h. Then a test line was demarcated and thinly blotted with 5 μ L of DVS solution (10% DVS, 5% DMF in 50-mM sodium carbonate, pH 10). Five blotting steps were performed with 10-min intervals between each step. The activated test line was then immediately blotted with 1 μ L of different amine-containing compounds (NH₂-PEG₂-biotin and NH₂-PEG₃-BCN, 1 mM each in pure water) for a total of five blotting steps with a 10-min drying interval at room temperature in between each step. The membranes were then blocked using blocking buffer (1.0% BSA, 0.1% Tween20 in 1x PBS, pH 7.4) for 3 h and subsequently rinsed with pure water. Membranes were prepared in duplicate for use in LFA and chemiluminescence analysis. NH₂-PEG₃-BCN was linked to the surface of nitrocellulose for use as an alkyne click handle²⁶ to N₃-PEG-biotin, which was blotted to the BCN-modified surface in the same amount and same manner as the NH₂-PEG₂-biotin control described previously. Chemiluminescence was measured by probing the strips with streptavidin-HRP (1:10,000 dilution in 1x PBS) and developing the signal with a SuperSignal West Femto substrate for 5 min before exposing and the capturing images.

3.5 LFA Preparation and Assembly

Prior to running an assay, both the sample pad and conjugate pad were saturated with buffer to prevent reporter aggregation throughout the test. The sample pad was saturated with sample pad buffer (0.1% BSA, 0.01% Tween20 in 1x PBS, pH 7.4), and the conjugate pad was saturated with conjugate pad buffer (1.0% BSA, 0.1% Tween20, 10% sucrose in 1x PBS, pH 7.4). Saturation was achieved by adding droplets of solution to the appropriate paper component with a micropipette until the paper was completely soaked. After saturation the pads were dried at 37 °C for

3–5 h until completely dry. After drying, the sample pad is ready for use. The conjugate pad must then be saturated with reporter conjugate for use in the assay (either functionalized AuNPs or red latex beads), and further dried an additional 3–5 h at 37 °C before being ready to use. All LFAs were run using 100- μ L LFA buffer (1.0% BSA, 0.1% Tween20 in 1x PBS, pH 7.4), which was deposited directly onto the sample pad of an assembled LFA to begin the assay.

3.6 Dipstick Assays

To rapidly screen for bead mobility and functionalization efficacy, dipstick assays were used. Briefly, a capture ligand is blotted onto the test line of a nitrocellulose strip and allowed to dry. It is then “dipped” into a well on a 96-well plate containing 50 μ L of modified reporter that will migrate up the strip and bind to the capture ligand. This method allows for the quick assessment of reporter and capture ligand interaction without the burden of complete LFA assembly.

4. Results and Discussion

Given that biotin, much like SBP, is a small compound with even higher affinity for streptavidin, experiments were frequently performed in tandem with a biotin control. This provides a means for measuring the impact of affinity on the setup. SBP was trialed at both the reporter interface and the test line surface to determine the extent of peptide binding when placed in different portions of the assay. Additionally, the efficacy of copper-free click chemistry (where an azide [R-N₃] and strained alkyne [C \equiv N] react to form a covalent bond through a triazole [Tz₄] linkage via 1,4 dipolar cycloaddition²⁶) was assessed at the test line surface. The general reaction scheme for copper-catalyzed click reaction is shown in Fig. 2.

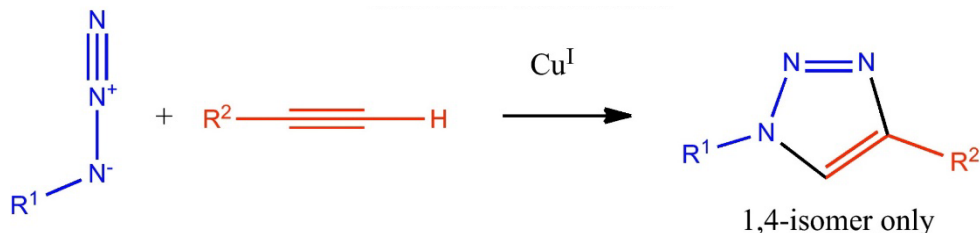


Fig. 2 General reaction scheme for a copper(I)-catalyzed click reaction

4.1 Covalent Immobilization of Biotin

Using DVS, NH₂-PEG₃-BCN was covalently linked to the test line to provide an alkyne handle for click chemistry. The reaction was then performed by adding N₃-PEG-biotin to generate NH₂-PEG₃-Tz₄-PEG-biotin at the surface. Additionally,

NH₂-PEG₂-biotin was also included as a control, and the biotin amounts were identical between click reaction and control to ensure both samples could be directly compared. This scheme was performed in duplicate to assess both LFA characteristics as well as to assess levels of biotin at the surface using a streptavidin-HRP probe, as shown in Fig. 3.

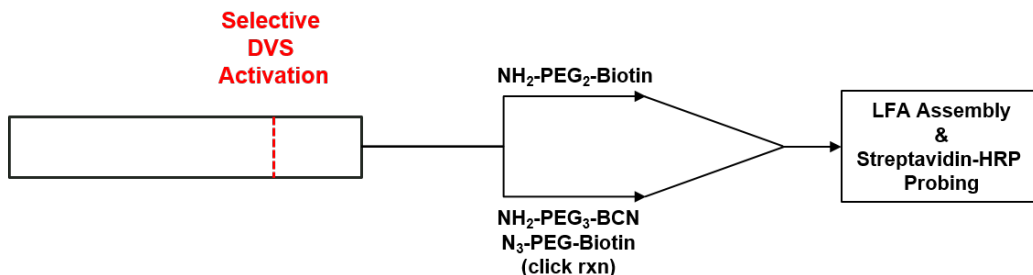


Fig. 3 General schematic depicting the pathway used for covalent modification at the test-line surface of nitrocellulose

Results are shown in Fig. 4. The chemiluminescence data demonstrated that covalent immobilization and surface click reaction provided better surface biotinylation than either of the adsorption controls. However, in both cases, surface biotin failed to capture the red-streptavidin reporter beads. This suggests that the amount of biotin linked to the surface was either not enough to bind streptavidin or was inaccessible for chemistry by the beads. These results prompted further investigation of passive adsorption.

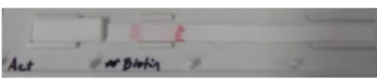
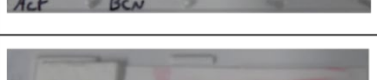
Ligand	Attachment	Lateral Flow	Chemiluminescence
NH ₂ -PEG ₂ -Biotin	Covalent		
	Adsorption (control)		
NH ₂ -PEG ₃ -Trz-PEG-Biotin	Covalent		
	Adsorption (control)		

Fig. 4 Results from the covalent immobilization of ligands and in situ click reaction at the test line of nitrocellulose using DVS. Chemiluminescence was measured after probing with streptavidin-HRP and developing the signal using a SuperSignal substrate.

4.2 Investigation of Passive Adsorption

To evaluate the necessity for a covalent linking mechanism, passive adsorption was further characterized. Several small biotinylated compounds were passively blotted at the test line and used to capture a red-streptavidin reporter. The compounds are listed in Table 1.

Table 2 Small compounds chosen to be passively adsorbed to the test line

Compound	MW (g/mol)
GTP-biotin	848
NHS-LC-biotin	556
HS-SBP	1011

As shown in Fig. 5, despite being relatively small compounds, all of the biotinylated ligands were able to successfully capture red-streptavidin latex beads. This suggests that the ability to capture ligands is independent of the size of the molecule adsorbed to the test line surface, and that the interaction between the reporter and capture agent will generate a positive signal so long as the adsorbed capture agent is deposited beyond the threshold concentration. The background smearing of the red-latex reporter was significantly higher than typical capture of red-streptavidin antibody; however, as the concentration of small ligand increases, the smearing becomes less prominent.

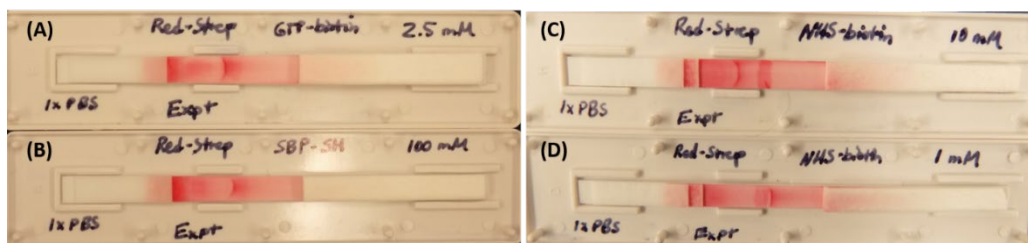


Fig. 5 Capture of red-streptavidin latex beads by small biotinylated molecules (MW < 1000 g/mol) that were passively adsorbed to the test-line surface: A) GTP-biotin at 2.5 mM, B) HS-SBP at 100 mM, C) NHS-biotin at 10 mM, and D) NHS-biotin at 1 mM

It was predicted that the net charge of the molecule had implications on the strength of adsorption to the test line. To evaluate this, the pH was screened from pH 5 to pH 9 using SBP and an anti-streptavidin antibody as capture ligands for a red-streptavidin reporter. Results are shown in Fig. 6. The antibody demonstrated similar capture of reporter throughout the pH range. HS-SBP on the other hand, showed promising capture at pH 7 and seemingly haphazard capture at all other pH values. This suggests that the ionization state of the adsorbed capture ligand has drastic effects on its ability to bind the reporter.

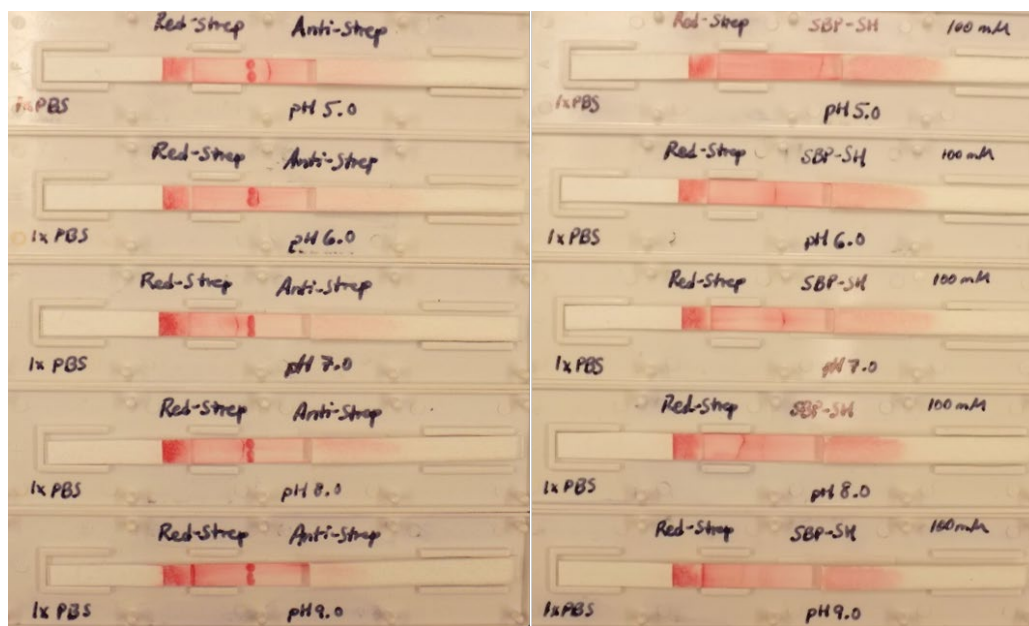


Fig. 6 Red-streptavidin latex beads captured by (left) an anti-streptavidin antibody and (right) HS-SBP ranging from pH 5 to pH 9 (top to bottom)

HS-SBP showed promising retention and binding at pH 6 and 7 when captured by red-streptavidin beads. To determine if the signal can be further increased using passive adsorption, a layering strategy was investigated. Briefly, test-line ligand was deposited in thin 1- μ L steps for a series of blotting events until a desired saturation was achieved. Layering was performed up to four times for HS-SBP and NHS-biotin at the test line and evaluated using red-streptavidin as the reporter. Results are shown in Fig. 7. Layering appears to be an effective strategy for increasing the load of capture agent at the test line. For both ligands the signal strength seemed to increase with increasing layers, and four layers visually captured more red-streptavidin reporter molecules than a single layer of deposition. Because of this result it was decided that passive adsorption was a reasonable mechanism for depositing SBP at the surface, and covalent modification methods at the test line were no longer being pursued.



Fig. 7 Layering of (left) NHS-biotin and (right) HS-SBP. A control is included in the first row (BSA at the test line for NHS-biotin and red-COOH unfunctionalized beads for HS-SBP). Stock concentrations were 10 and 100 mM for NHS-biotin and HS-SBP, respectively. Layering is shown from one to four layers (top to bottom).

4.3 Characterization of Red-Carboxylate Latex Beads

Red-carboxylate beads were functionalized with SBP using EDC–NHS coupling and were used to detect 1- μ M streptavidin in a sandwich assay using anti-streptavidin antibody as the capture agent, shown in Fig. 8. This demonstrates that the N-terminus of peptides can be covalently linked to red latex beads without interference of binding to the intended target. Note SBP does not contain any lysine residues, thus facilitating the use of EDC–NHS coupling.

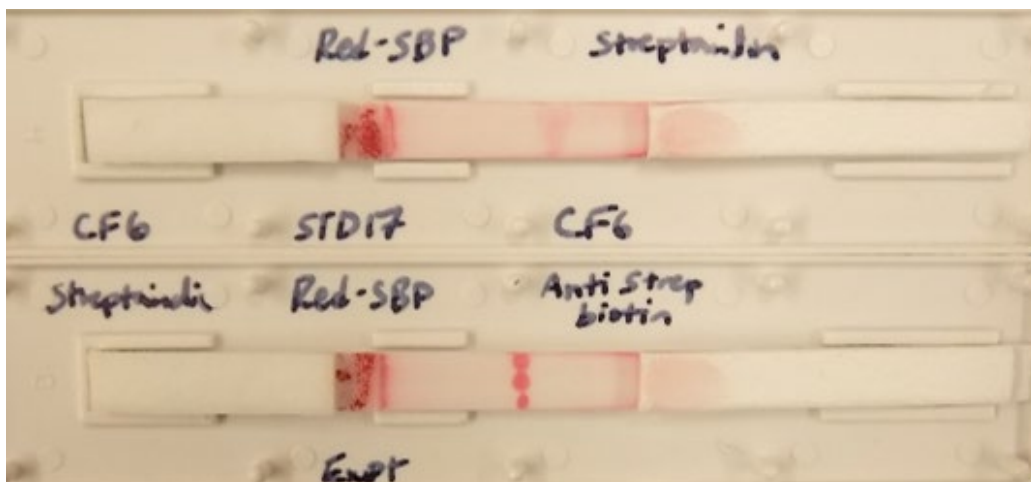


Fig. 8 (top) Streptavidin used to capture red-SBP reporter deposited at 187 μ M. (bottom) Sandwich assay detecting streptavidin at 1 μ M using a red-SBP reporter and anti-streptavidin antibody as the capture agent.

During the characterization of red latex beads, it was noticed that the carboxylate beads would bind to seemingly random targets and demonstrated many false positives. This prompted testing of many different ligands against native, unmodified carboxylate beads to determine the etiology of nonspecific binding. The ligands used at the test line include anti-streptavidin, streptavidin, HS-SBP, nonstructured protein1-His₆ (nSP1-His₆), catabolite control protein A-His₆ (CcpA-His₆), and HPr Kinase-His₆ (HprK-His₆). Note His₆ refers to a poly-histidine tag used for affinity purification. The native beads likely bind the affinity tag through a charge interaction, as shown in Fig. 9.



Fig. 9 Evaluation of nonspecific binding by native, unmodified carboxylate beads. Native beads appear to have affinity for His-tagged constructs (right).

The promiscuous binding to His-tagged constructs presented new challenges with using red latex beads in the LFA. His-tag affinity purification plays a critical role in the production of PCCs. Therefore, several measures were studied in attempts to mitigate the nonspecific binding. It was presumed that the binding event between

the red carboxylate beads and the His-tag was primarily mediated through electrostatic interactions. The nonspecific signal was evaluated at from pH 2 through pH 12. Additionally, if the mechanism for binding was through a pocket of some sort, we also incorporated imidazole and divalent cations (CaCl_2 and CoCl_2) to potentially inhibit the interaction competitively. Results for the quenching attempts are shown in Figs. 10–12.



Fig. 10 Evaluation of nonspecific binding of native red carboxylate beads to a His-tagged construct from (left) pH 2 through pH 6, and (right) pH 7 through pH 12

Screening through a wide pH range revealed prevention of nonspecific binding only at the extremes, pH 2 and 12. For applications beyond nonspecific binding, these extreme pH values would likely denature target, thus making pH a parameter that does not avert nonspecific binding.

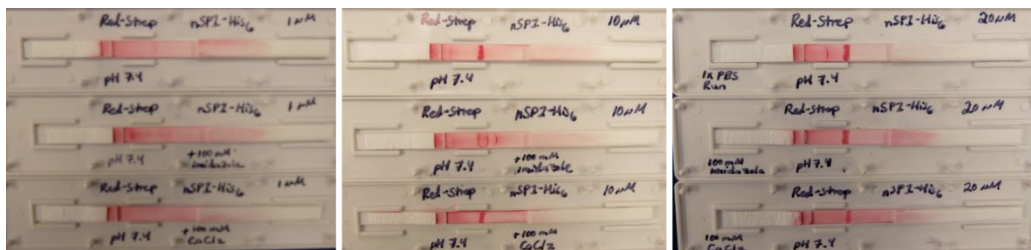


Fig. 11 Evaluation of various measures taken to mitigate nonspecific binding of red latex beads to a His-tagged construct. (left to right) Each column consists of nSP1-His6 at 1, 10, and 20 μM . The top row is a control, the middle row includes the addition of 100-mM imidazole, and the bottom row includes the addition of 100-mM CaCl_2 .



Fig. 12 Prevention of nonspecific binding of unmodified native latex beads to CcpA-His₆ using cobalt(II) chloride as a divalent cation inhibitor at (top to bottom) 100, 500, and 1.0 M

As shown in Figs. 10–12, attempts at quenching the nonspecific binding event of red carboxylate beads to His-tagged constructs was unsuccessful. Because the development process for PCCs involves the use of His-tags for affinity purification of targets, it is necessary to investigate reporters that do not demonstrate promiscuity and potential off-target effects. Thus, red latex beads were no longer being considered as a reporter for the LFA.

4.4 Characterization of AuNPs

AuNPs were investigated as a reporter for use in the LFA after red carboxylate latex beads were ruled out due to issues with nonspecific binding to His-tagged constructs. Among the first characterization tests performed with AuNPs included the use of citrate-capped native AuNPs against various poly-histidine proteins to ensure there is no nonspecific interaction, results of which (shown in Fig. 13) demonstrate persistent nonspecific binding to one of the His-tagged constructs.

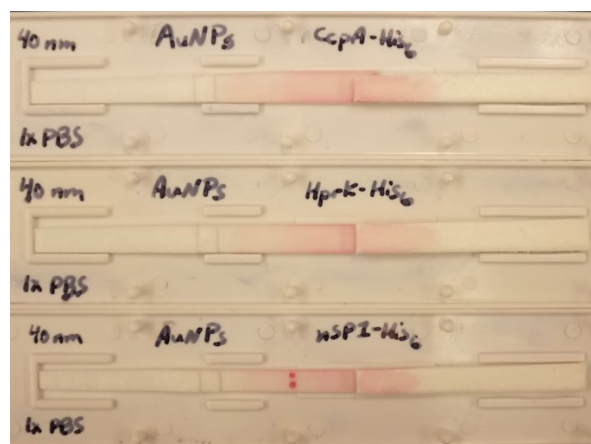


Fig. 13 Capture of citrate-capped native 40-nm AuNPs using CcpA-His₆, HprK-His₆, and nSP1-His₆

Of the three different His-tagged constructs, citrate-capped AuNPs demonstrated nonspecific binding only to nSP1-His₆. Structural investigation revealed that nSP1-His₆ contains 16 cysteine residues, while the other two constructs (CcpA-His₆ and HprK-His₆) do not contain any cysteine residues. It is likely that the nonspecific binding is due to interaction with the thiol group in cysteine. We therefore predicted that promiscuous binding would be inhibited upon functionalization with ligands containing PEG, which is well-characterized in the literature to be an excellent AuNP stabilizer and can densely pack the surface of gold.²⁷

Initial functionalization efforts were focused on producing biotinylated AuNPs using HS-PEG-biotin MW5000. This required a few optimization steps to maintain AuNP stability throughout modification. Specifically, to determine the optimum ligand concentration for AuNP functionalization, various concentrations of ligand were mixed with AuNPs at OD₅₃₀ = 3. Then a fixed volume of 1% sodium chloride (NaCl) was added to each sample. The absorbance at 530 nm was measured before and after the addition of NaCl. The concentration of ligand corresponding to the smallest difference in before and after UV-visual measurements was chosen as the functionalization concentration. The same optimization described previously was also performed for pH with native AuNPs. For HS-PEG-biotin MW5000, the optimum functionalization was determined to be at 0.5 mg/mL at pH 8, as shown in Fig. 14.

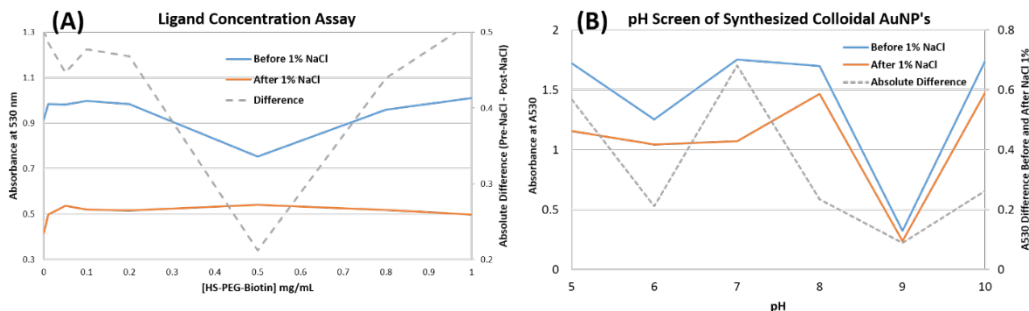


Fig. 14 A) Ligand concentration screen for functionalization of AuNPs with HS-PEG-biotin MW5000. B) pH stability screen of native AuNPs.

AuNPs were functionalized with HS-PEG-biotin MW5000 at the optimized conditions (0.5 mg/mL at pH 8) overnight and evaluated using streptavidin as the capture agent. Results are shown in Fig. 15. Streptavidin captured the biotinylated AuNP reporter at 187 μ M; however, the signal was lost at 18.7 μ M. For the sandwich assays, anti-streptavidin antibody captured the streptavidin–reporter complex at 1 μ M, whereas SBP failed to capture the streptavidin–reporter complex, suggesting substrate accessibility issues or low amounts of SBP adsorbed to the surface.



Fig. 15 Capture of AuNP-S-PEG-biotin MW5000 reporter using (top to bottom) streptavidin at 187 μ M, streptavidin at 18.7 μ M, sandwich assay detecting 1- μ M streptavidin using anti-streptavidin as a capture agent, and sandwich assay detecting 1- μ M streptavidin using SBP as a capture agent

To evaluate the extent of blocking ability and ensure that intended targets were not being quenched, a comprehensive study was performed to assess the effect of

various ligand:blocker ratios on the reporter–test-line interaction. Specifically, two ligands (HS-SBP and HS-PEG-biotin MW1000) and four blockers (HS-PEG-COOH MW5000 and MW10,000, MUDA, and β ME) were mixed at different ligand:blocker ratios while maintaining a fixed blocker ρ_{packing} of 1.25 molecules/nm². These were captured by nSP1-His₆ to assess nonspecific binding in addition to being captured by streptavidin to evaluate intended binding. Results are shown in Figs. 16 and 17.

(A)		nSP1 Capture (9.4 μM)		
		Ligand:Blocker		
Ligand	Blocker	0.5:1	1:1	5:1
HS-PEG-Biotin 1000	MUDA			
	HSPEG5k			
	HSPEG10k			
	β -ME			
(B)		Streptavidin Capture (200 μM)		
		Ligand:Blocker		
Ligand	Blocker	0.5:1	1:1	5:1
HS-PEG-Biotin 1000	MUDA			
	HSPEG5k			
	HSPEG10k			
	β -ME			

Fig. 16 A) Evaluation of nonspecific binding to nSP1-His₆ by AuNP-S-PEG-biotin MW1000 using various blockers and ligand:blocker ratios. B) Evaluation of intended target binding using streptavidin as a capture agent to bind AuNP-S-PEG-biotin MW1000 using those same blockers and ligand:blocker ratios.

(A)		nSP1 Capture (9.4 μ M)		
		Ligand:Blocker		
Ligand	Blocker	0.5:1	1:1	5:1
HS-SBP	MUDA			
	HSPEG5k			
	HSPEG10k			
	β -ME			

(B)		Streptavidin Capture (200 μ M)		
		Ligand:Blocker		
Ligand	Blocker	0.5:1	1:1	5:1
HS-SBP	MUDA			
	HSPEG5k			
	HSPEG10k			
	β -ME			

Fig. 17 A) Evaluation of nonspecific binding to nSP1-His₆ by AuNP-S-SBP using various blockers and ligand:blocker ratios. B) Evaluation of intended target binding using streptavidin as a capture agent to bind AuNP-S-SBP using those same blockers and ligand:blocker ratios.

All four blockers appear to be effective at preventing nonspecific binding to nSP1-His₆. Both AuNP-biotin MW1000 and AuNP-SBP begin to aggregate upon increasing the ligand:blocker ratio to 5:1 while using MUDA and β ME as the blockers, as evidenced by the lack of mobility in the dipstick. The results herein suggest that increasing the PEG linker length in the presence of an appropriate blocking ligand helps facilitate stable functionalization and provides an arm for ligand accessibility.

5. Conclusion

It is likely that using a long PEG linker on both the reporter AuNPs and the test line will enable successful incorporation of other peptides and non-Ig reagents into the LFA. Specifically, it may be fruitful to consider adding an N- or C-terminal thiolated PEG linker during the peptide synthesis to allow for simple AuNP modification. This may also have a positive impact on the passive adsorption of ligands at the test line as well. The results presented in this report provide a foundation for future experiments. More investigation is required to fully develop a robust biosensing platform using non-Ig affinity ligands as the substrate for detection.

6. References

1. Tsai T-T, Huang T-H, Ho NY-J, Chen Y-P, Chen C-A, Chen C-F. Development of a multiplex and sensitive lateral flow immunoassay for the diagnosis of periprosthetic joint infection. *Sci Rep.* 2019;9:2–9.
2. Prentice KW, DePalma L, Ramage JG, Sarwar J, Parameswaran N, Peteresen J, Yockey B, Young J, Joshi M, Thirunawukarasu, N, et al. Comprehensive laboratory evaluation of a lateral flow assay for the detection of *Yersinia pestis*. *Heal Secur.* 2019;17:439–453.
3. Kamphee H, Chaiprasert A, Prammananan T, Wiriyaichaiyorn N, Kanchanatavee A, Dharakul T. Rapid molecular detection of multidrug-resistant tuberculosis by PCR-nucleic acid lateral flow immunoassay. *PLoS One* 10. 2015:1–17.
4. Apilux A, Rengpipat S, Suwanjang W, Chailapakul O. Development of competitive lateral flow immunoassay coupled with silver enhancement for simple and sensitive salivary cortisol detection. *EXCLI J.* 2018;17:1198–1209.
5. Choi JR, Yong KW, Choi JY, Cowie AC. Emerging point-of-care technologies for food safety analysis. *Sensors.* 2019;19:1–31.
6. O’Farrell B. Evolution in lateral flow-based immunoassay systems. In: *Lateral flow immunoassay*. Totawa (NJ): Humana Press Inc.; 2009.
7. Sajid M, Kawde AN, Daud M. Designs, formats and applications of lateral flow assay: a literature review. *J Saudi Chem Soc.* 2015;19:689–705.
8. Hsieh HV, Dantzler JL, Weigl BH. Analytical tools to improve optimization procedures for lateral flow assays. *Diagnostics.* 2017;7:29.
9. Škrlec K, Štrukelj B, Berlec A. Non-immunoglobulin scaffolds: a focus on their targets. *Trends Biotechnol.* 2015;33:408–418.
10. Simeon R, Chen Z. In vitro-engineered non-antibody protein therapeutics. *Protein Cell.* 2018;9:3–14.
11. Richards DA. Exploring alternative antibody scaffolds: antibody fragments and antibody mimics for targeted drug delivery. *Drug Discov Today Technol.* 2018;30:35–46.
12. Kyle S. Affimer proteins: theranostics of the future? *Trends Biochem Sci.* 2018;43:230–232.

13. Klont F, Hadderingh M, Horvatovich P, Ten Hacken NHT, Bischoff R. Affimers as an alternative to antibodies in an affinity LC-MS assay for quantification of the soluble receptor of advanced glycation end-products (srage) in human serum. *J Proteome Res.* 2018;17:2892–2899.
14. Koide S, Huang J. Generation of high-performance binding proteins for peptide motifs by affinity clamping. *Methods Enzymol.* 2013;523:285–302.
15. Thiviyanathan V, Gorenstein DG. Aptamers and the next generation of diagnostic reagents. *Proteomics - Clin Appl.* 2012;6:563–573.
16. Silverman J, Liu Q, Bakker A, To W, Duquay A, Alba BM, Smith R, Rivas A, Li P, Le H, et al. Multivalent avimer proteins evolved by exon shuffling of a family of human receptor domains. *Nat Biotechnol.* 2005;23:1556–1561.
17. Stumpp MT, Binz HK, Amstutz P. DARPins: a new generation of protein therapeutics. *Drug Discov Today* 2008;13:695–701.
18. Kadonosono T, Yimchuen W, Ota Yumi, See K, Furuta T, Shiozawa T, Kitazawa M, Goto Y, Patil A, Kuchimaru T, et al. Design strategy to create antibody mimetics harbouring immobilised complementarity determining region peptides for practical use. *Sci Rep.* 2020;10:891.
19. Sha F, Salzman G, Gupta A, Koide S. Monobodies and other synthetic binding proteins for expanding protein science. *Protein Sci.* 2017;26:910–924.
20. Coppock MB, Warner CR, Dorsey B, Orlicki JA, Sarkes DA, Lai BT, Pitram SM, Rhode RD, Malette J, Wilson JA, et al. Protein catalyzed capture agents with tailored performance for in vitro and in vivo applications. *Pept Sci.* 2017;1–13.
21. Coppock MB, Sarkes DA, Hurley MM, Stratis-Cullum DN. Peptide-based antibody alternatives for biological sensing in austere environments. *Proc SPIE.* 2017;10081.
22. Holstein CA, Chevalier A, Bennett S, Anderson CE, Keniston K, Olsen C, Li B, Bales B, Moore DR, Fu E, et al. Immobilizing affinity proteins to nitrocellulose: a toolbox for paper-based assay developers. *Anal Bioanal Chem.* 2016;408:1335–1346.
23. Coppock MB, Stratis-Cullum DN. A universal method for the functionalization of dyed magnetic microspheres with peptides. *Methods.* 2019;158:12–16.

24. Kozłowski R, Ragupathi A, Dyer RB. Characterizing the surface coverage of protein–gold nanoparticle bioconjugates. *Bioconjug Chem.* 2018;29:2691–2700.
25. Lauritzen E, Masson M, Rubin I, Holm A. Dot immunobinding and immunoblotting of picogram and nanogram quantities of small peptides on activated nitrocellulose. *J Immunol Methods* 1990;131:257–267.
26. Kolb HC, Finn MG, Sharpless KB. Click chemistry: diverse chemical function from a few good reactions. *Angew Chemie Int Ed.* 2001;40:2004–2021.
27. Gao J, Huang X, Liu H, Zan F, Ren J. Colloidal stability of gold nanoparticles modified with thiol compounds: bioconjugation and application in cancer cell imaging. *Langmuir.* 2012;28:4464–4471.

List of Symbols, Abbreviations, and Acronyms

aa	amino acid
AuNP	gold nanoparticle
BCN	bicyclononyne
β ME	beta-mercaptoethanol
BSA	bovine serum albumin
CaCl ₂	calcium chloride
CcpA	control catabolite protein A
CoCl ₂	cobalt chloride
COOH	carboxylate
DARPin	designed ankyrin repeat protein
DMF	N,N-dimethylformamide
DMSO	dimethyl sulfoxide
DNA	deoxyribonucleic acid
DVS	divinyl sulfone
EDC	1-ethyl-3-(3-dimethylaminopropyl)carbodiimide
GTP	guanosine triphosphate
HRP	horseradish peroxidase
HAuCl ₄	hydrogen tetrachloroaurate(III) hydrate
HprK	Hpr kinase
LFA	lateral flow assay
MES	2-(N-morpholino)ethanesulfonic acid
MUDA	mecaptoundecanoic acid
MW	molecular weight
N ₃	azide
NaCl	sodium chloride

NaCt	sodium citrate trihydrate
NH ₂	amine
NHS	N-hydroxysulfosuccinimide
non-Ig	nonimmunoglobulin
nSP1-His6	nonstructured protein 1
PBS	phosphate buffered saline
PEG	polyethylene glycol
PCC	protein-catalyzed capture agent
POC	point of care
RNA	ribonucleic acid
SBP	streptavidin binding peptide
HS-SBP	thiolated streptavidin binding peptide
Tz ₄	triazole
UV	ultraviolet

1 DEFENSE TECHNICAL
(PDF) INFORMATION CTR
DTIC OCA

1 CCDC ARL
(PDF) FCDD RLD CL
TECH LIB

4 CCDC CBC
(PDF) CHEMICAL BIOLOGICAL CTR
S BROOMALL
E HOFMANN
S SOZHAMANNAN
M RETFORD

10 CCDC ARL
(PDF) FCDD RLS
D STRATIS-CULLUM
K KRAPELS
M WRABACK
G BRILL
V ATKINSON
FCDD RLS C
J SUMNER
C COOPER
FCDD RLS CB
M COPPOCK
A WINTON
S LIU